

# Articles

## NMR Spectral Assignment and Determination of the Bridge Reversal Barrier in 3-*n*-Butyl-[3]-trithiaferrocenophane

Eric R. Johnston<sup>\*,†</sup> and Paul F. Brandt<sup>‡</sup>

*Department of Chemistry, The University of North Carolina at Greensboro, Greensboro, North Carolina 27412, and Department of Chemistry and Physics, Western Carolina University, Cullowhee, North Carolina 28723*

Received December 11, 1997

The high barrier to reversal of the bent trisulfide bridge in 3-*n*-butyl-[3]-trithiaferrocenophane results in syn and anti stereoisomers which are distinguishable by NMR at 300 K. All seven ring hydrogen atoms and their directly attached carbon atoms in each stereoisomer are nonequivalent and have been uniquely assigned using a suite of one- and two-dimensional experiments. Row slices of the total correlation (TOCSY) spectrum provide the individual ring <sup>1</sup>H NMR subspectra. The two ring proton sets of each stereoisomer can be correlated via inter-ring nuclear Overhauser effects across the iron atom of the sandwich. The syn and anti isomers are in a slow dynamic equilibrium brought about by reversal of the trisulfide bridge, which interconverts the hydrogen-atom pairs in the two stereoisomers. The rate of this process has been measured with high accuracy by 2D exchange spectroscopy. The rate constant  $k = 0.07 \text{ s}^{-1}$  at 300 K corresponds to an activation barrier of 19.1 kcal/mol, virtually identical with that of the unsubstituted parent compound. Apparently, the *n*-butyl group at the 3-position exerts no significant steric or inductive effect on the bridge reversal rate, which is enthalpically driven.

### Introduction

Since their discovery in 1969,<sup>1</sup> the trichalcogen-[3]-ferrocenophanes have been extensively studied. Of particular interest to us are the barriers to bridge reversal in these compounds, the mechanism by which this occurs, and the effect of ring substituents on the reversal rate. The existence of a fluxional bridge reversal process in these compounds has been known for some time.<sup>2–4</sup> The pyramidal nature of the bridge leads to regioisomerism in ferrocenophanes bearing substituents, and a number of NMR studies of such compounds have been reported.<sup>5–9</sup> We report here the results of a series of NMR investigations leading to the

complete assignment of the <sup>1</sup>H spectrum of 3-*n*-butyl-[3]-trithiaferrocenophane and the accurate measurement of the bridge reversal barrier using two-dimensional exchange spectroscopy.

### Results

**Assignment of the <sup>1</sup>H and <sup>13</sup>C NMR Spectra.** The ferrocenyl region of the <sup>1</sup>H NMR spectrum of 3-*n*-butyl-[3]-trithiaferrocenophane measured in toluene-*d*<sub>6</sub> at 300 K is shown in Figure 1. Fourteen distinct multiplets may be observed, numbered consecutively from high to low frequency. The compound exists as a 1:1 mixture of the syn and anti stereoisomers, with the pyramidal trisulfide bridge proximal to and distal from the 3-*n*-butyl substituent, respectively, as depicted in Figure 2. Due to the 3-*n*-butyl group, all seven hydrogen atoms in each stereoisomer are nonequivalent, giving rise to 14 resonances. This observation additionally indicates that the syn and anti isomers are interconverting very slowly and that the bridge reversal barrier is quite high. Also visible in the <sup>1</sup>H NMR spectrum are weak ring proton multiplets due to ca. 15% of the 2-*n*-butyl isomer, which exists as a 1:2 syn:anti mixture, the anti form being favored for steric reasons.<sup>10</sup>

<sup>†</sup> The University of North Carolina at Greensboro.

<sup>‡</sup> Western Carolina University.

(1) Davison, A.; Smart, J. C. *J. Organomet. Chem.* **1969**, *19*, P7.

(2) Davison, A.; Smart, J. C. *J. Organomet. Chem.* **1979**, *174*, 321.

(3) Abel, E. W.; Booth, M.; Orrell, K. G. *J. Organomet. Chem.* **1980**, *186*, C37.

(4) Abel, E. W.; Booth, M.; Orrell, K. G. *J. Organomet. Chem.* **1981**, *208*, 213.

(5) Butler, I. R.; Cullen, W. R.; Herring, F. G.; Jagannathan, N. R.; Einstein, F. W. B.; Jones, R. *Inorg. Chem.* **1986**, *25*, 4534.

(6) Butler, I. R.; Cullen, W. R. *Can. J. Chem.* **1989**, *67*, 1851.

(7) Galloway, C. P.; Rauchfuss, T. B. *Angew. Chem. Intl. Ed. Engl.* **1993**, *32*, 1319.

(8) Compton, D. L.; Rauchfuss, T. B. *Organometallics* **1994**, *13*, 4367.

(9) Abel, E. W.; Long, N. J.; Orrell, K. G.; Sik, V.; Ward, G. N. *J. Organomet. Chem.* **1993**, *462*, 287.

(10) Piorko, A.; Ratajczak, A. *Org. Magn. Reson.* **1981**, *16*, 312.

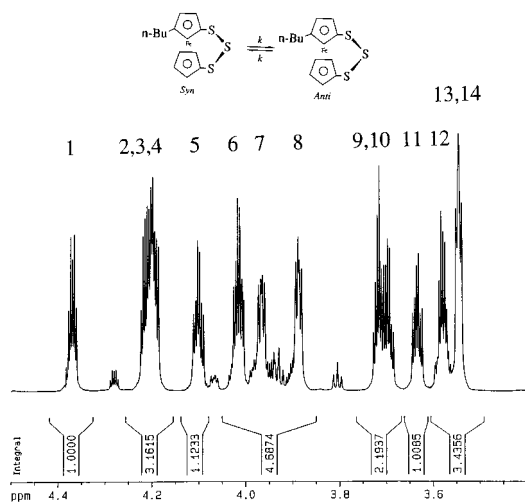


**Figure 1.**  $^1\text{H}$  NMR spectrum of the ring protons of 3-*n*-butyl-[3]-trithiaferrocenophane recorded at 300 MHz and 300 K in toluene- $d_8$ . The protons have been numbered consecutively from high to low frequency.

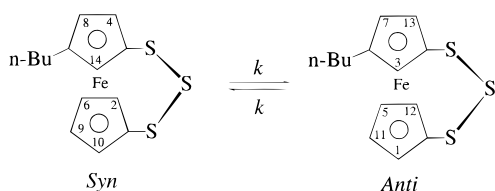


**Figure 2.** Syn/anti bridge inversion and ring proton spectral assignments for 3-*n*-butyl-[3]-trithiaferrocenophane.

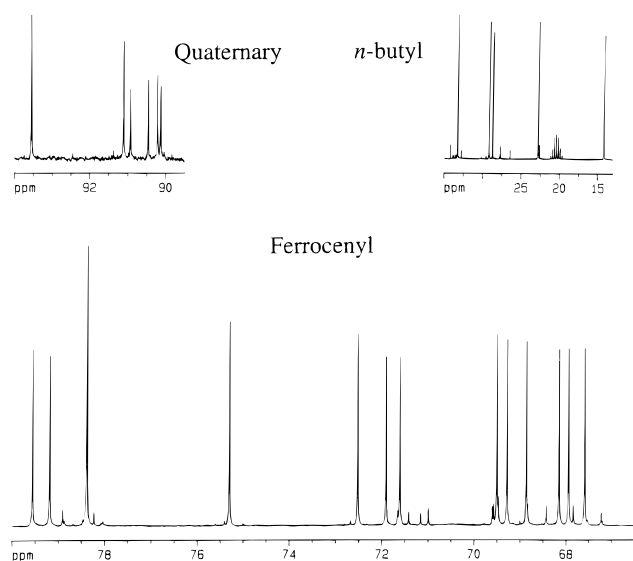


**Figure 3.**  $^{13}\text{C}$  NMR spectrum of 3-*n*-butyl-[3]-trithiaferrocenophane recorded at 75 MHz and 300 K in toluene- $d_8$  with line broadening of 1 Hz. A doubling of the resonances is apparent with the signals at  $\delta$  78.4 overlapped.

The  $^{13}\text{C}$  spectrum shown in Figure 3 also reveals a doubling of the  $^{13}\text{C}$  signals owing to syn/anti isomerism. The ferrocenyl carbon atoms are correlated to their directly attached hydrogen atoms in the  $^1\text{H}$ - $^{13}\text{C}$  chemical shift correlation experiment of Figure 4, which clearly reveals fourteen correlation peaks. The carbon atom resonating at  $\delta$  79.53 bears  $\text{H}_1$ , whereas its neighbor at  $\delta$  79.15 bears  $\text{H}_3$ , for example. The four  $^{13}\text{C}$  resonances in the frequency region  $\delta$  78–80 are assignable to carbon atoms adjacent to the trisulfide bridge

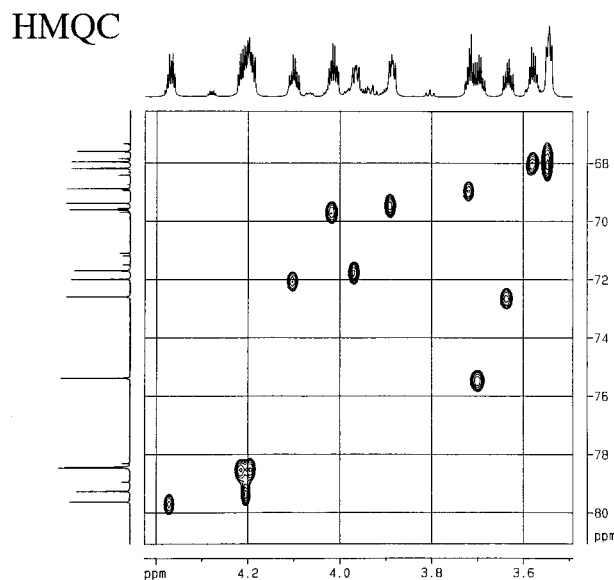


**Figure 4.** Inverse-detected  $^1\text{H}$ - $^{13}\text{C}$  chemical shift correlation spectrum of the ferrocenyl region of 3-*n*-butyl-[3]-trithiaferrocenophane. Fourteen correlation peaks are visible. The  $^{13}\text{C}$  projection has been resolution enhanced to resolve the signals at  $\delta$  78.4.

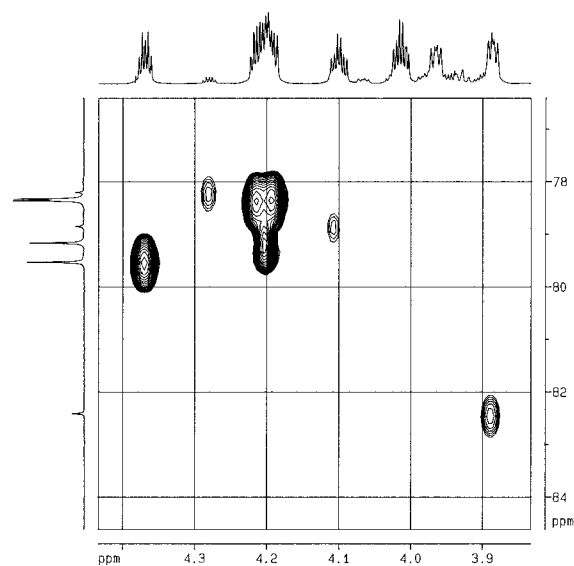


**Figure 5.** Expansion of Figure 4, illustrating  $^1\text{H}$ - $^{13}\text{C}$  correlation signals originating from the minor 2-*n*-butyl isomer.

in the two stereoisomers,<sup>10</sup> although it is not possible at this point to determine whether they are the four carbon atoms distal to the bridge or proximal to it.

Also present in the chemical shift correlation expansion shown in Figure 5 are three correlation peaks attributable to protonated ring carbon atoms adjacent to the trisulfide bridge in the minor 2-*n*-butyl isomer (the fourth position being occupied by the *n*-butyl group). The  $^{13}\text{C}$  signal at  $\delta$  82.42 is significantly stronger than the other two at  $\delta$  78.87 and  $\delta$  78.19, which are of similar intensity. These signals are therefore assignable to carbon atoms *distal* to the bridge in the 1,2-isomer, with the signal at  $\delta$  82.42 originating from the single carbon atom in the more abundant anti isomer, as illustrated in Figure 6. Assignment to proximal carbon atoms would result in two strong resonances (anti) and one weak resonance (syn), the opposite of that

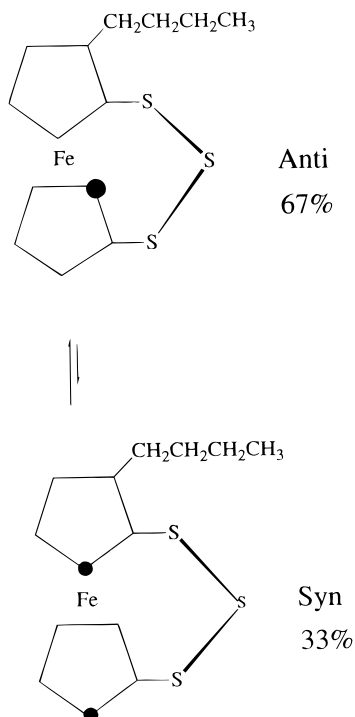


**Figure 6.** Syn/anti equilibrium for the 2-*n*-butyl isomer with the strong and weak correlation signals of Figure 5 indicated.

observed. On this basis, we assign the four  $^{13}\text{C}$  signals of the 1,3-isomer in the  $\delta$  78–80 region of the  $^{13}\text{C}$  spectrum to carbon atoms adjacent to and *distal* to the trisulfide bridge.

The carbon singlet resonating at  $\delta$  79.15 in the  $^1\text{H}$ -decoupled  $^{13}\text{C}$  spectrum appears as a doublet of quintets in the  $^1\text{H}$ -coupled  $^{13}\text{C}$  spectrum (not shown). The quintet structure arises from comparable three-bond couplings to two ring hydrogen atoms and to the  $\alpha$ -hydrogen atoms of the *n*-butyl substituent ( $^3J_{\text{C-H}} \approx 4$  Hz). Thus, this signal may be uniquely assigned to the carbon atom which is *adjacent to sulfur and the n-butyl group and distal to the bridge*. The  $^1\text{H}$ - $^{13}\text{C}$  chemical shift correlation spectrum of Figure 4 demonstrates that it correlates with  $\text{H}_3$  of Figure 1, so that  $\text{H}_3$  is uniquely assigned to the anti isomer, as indicated in the numbering scheme of Figure 2.

With  $\text{H}_3$  thus assigned, the  $^1\text{H}$  NMR spectrum may be factored into the subspectra for the individual rings of each isomer with a TOCSY experiment. Figure 7 displays one-dimensional row slices of the 2D TOCSY spectrum, clearly indicating two three-spin subsystems [3–7–13] and [4–8–14] and two four-spin subsystems [1–5–11–12] and [2–6–9–10]. The [4–8–14] subsystem is assigned to the substituted ring of the syn isomer, as indicated in Figure 2, but it is not yet possible to discern the sequential order of the protons within a given subsystem nor to decide which four-spin system is assignable to which stereoisomer. Nuclear Overhauser effect spectroscopy (NOESY) provides this additional information, permitting the complete ring  $^1\text{H}$  assignment and, hence, the complete ring  $^{13}\text{C}$  assignment from the chemical shift correlation spectrum of Figure 4.

The  $^1\text{H}$  NOESY spectrum of the ferrocenyl region measured at 300 K with a mixing time of 2.5 s is

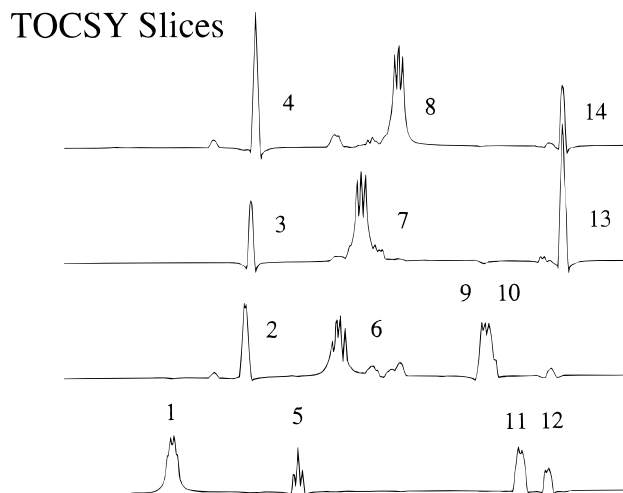


**Figure 7.** One-dimensional row slices of the two-dimensional TOCSY spectrum recorded in toluene- $d_6$  at 300 K with the individual ring proton subspectra labeled.

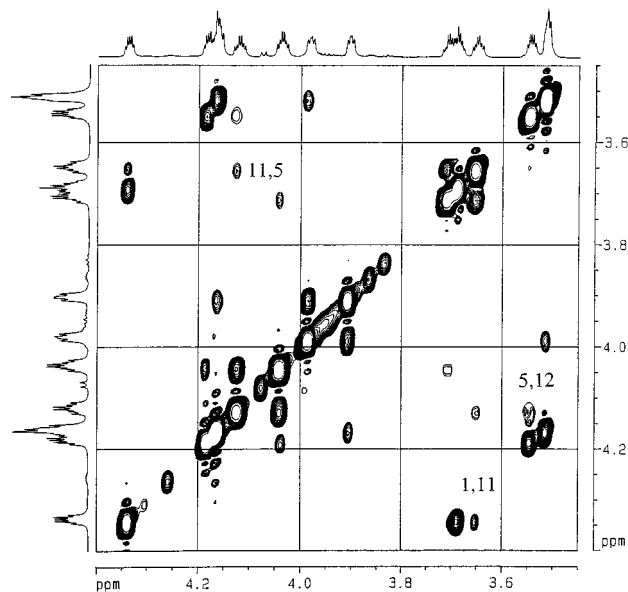


**Figure 8.** Two-dimensional NOESY spectrum recorded in toluene- $d_6$  at 300 K with a mixing time of 2.5 s. The (negative) NOE cross peaks of the [1–11–5–12] spin system are indicated.

illustrated in Figure 8. Both weak and strong cross peaks are evident, the former originating from nuclear Overhauser effects (negative in intensity) due to spatial proximity and the latter due to chemical exchange resulting from bridge reversal (positive in intensity). The NOE cross peaks permit the sequential assignments of Figure 2 as depicted in Figure 8 for the [1–11–5–12] subsystem. The numbering in Figure 2 for these protons is as shown and not the reverse as  $\text{H}_1$  and  $\text{H}_2$  correlate in Figure 4 with carbons *distal* to the trisulfide bridge. For the three-spin systems [3–7–13] and [4–8–14],  $\text{H}_7$  and  $\text{H}_{13}$  display NOE cross peaks as do  $\text{H}_4$  and  $\text{H}_8$  so that these pairs must be adjacent on their respective rings in the syn and anti stereoisomers. It is not possible at this point to determine which proton of each pair is adjacent to the *n*-butyl group nor is it possible to determine whether the [1–11–5–12] spin system belongs to the syn or anti isomer.

This information is contained in the NOESY expan-

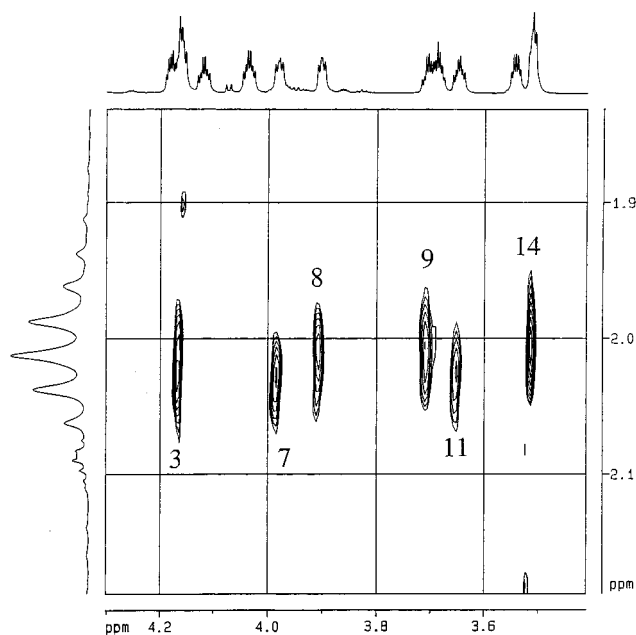


**Figure 9.** Expansion of the *n*-butyl  $\alpha$ -CH<sub>2</sub>/ring proton region of the NOESY spectrum of Figure 8, indicating the [3–7–11] and [8–9–14] subsystems of the anti and syn isomers, respectively.

**Table 1.** Tabulation of the Ring Proton and Carbon Chemical Shifts for the Syn and Anti Isomers, Using the Numbering Scheme of Figure 2

ring position	<sup>1</sup> H shift ( $\delta$ )	<sup>13</sup> C shift ( $\delta$ )
1	4.37	79.53
2	4.21	78.36
3	4.20	79.15
4	4.19	78.33
5	4.10	71.90
6	4.01	69.51
7	3.97	71.60
8	3.89	69.29
9	3.72	68.80
10	3.69	75.28
11	3.63	72.50
12	3.58	67.87
13	3.54	68.09
14	3.53	67.52

sion of Figure 9, which displays NOE cross peaks between the  $\alpha$ -hydrogen atoms of the *n*-butyl side chain and ring protons. The peaks fall into two categories, namely, [3–7–11] and [8–9–14], separated in the  $\omega_1$  dimension by the small but discernible chemical shift difference of the  $\alpha$ -hydrogen atoms of the stereoisomers. Thus, in the anti isomer, H<sub>3</sub> and H<sub>7</sub> flank the *n*-butyl group, with H<sub>11</sub> located directly below the  $\alpha$ -hydrogens of the side chain, whereas in the syn isomer, H<sub>8</sub> and H<sub>14</sub> flank the *n*-butyl group with H<sub>9</sub> directly beneath the side chain. The complete signal assignments of the ring protons and their directly attached carbon atoms are listed in Table 1 using the numbering scheme of Figure 2. The proton assignments are consistent with our observation that the longitudinal relaxation rate of the six ring protons flanked by two other ring protons or another ring proton and the *n*-butyl substituent (H<sub>5</sub>–H<sub>8</sub>, H<sub>9</sub>, and H<sub>11</sub>) is about 40% greater than the longitudinal relaxation rate of the eight ring protons adjacent to only one other ring proton or adjacent only to the *n*-butyl substituent (H<sub>1</sub>–H<sub>4</sub>, H<sub>10</sub>, H<sub>12</sub>–H<sub>14</sub>). We

**Table 2.** Chemical Exchange Diagonal and Cross Peak Volumes Measured at 300, 310, and 320 K, with the Corresponding Rate Constant *k* and Activation Free Energy

<i>T</i> (K)	<i>a<sub>d</sub></i>	<i>a<sub>x</sub></i>	$\tau_m$ (s)	<i>k</i> (s <sup>-1</sup> )	$\Delta G^\ddagger$ (kcal/mol)
300	478	84	2.5	0.07	19.2
310	646	278	2.0	0.23	19.1
320	794	553	1.5	0.57	19.2

have measured these rates to be 0.35 and 0.25 s<sup>-1</sup>, respectively, at 300 K.

**Measurement of the Bridge Reversal Rate.** In addition to the (negative) NOE cross peaks in Figure 8 resulting from spatial proximity of proton pairs within a given stereoisomer, large (positive) chemical exchange cross-peaks resulting from slow reversal of the trisulfide bridge are seen to connect proton pairs between the stereoisomers. Thus, H<sub>1</sub> and H<sub>10</sub> are connected, as are H<sub>5</sub> and H<sub>6</sub>, and so on. The amplitudes of the diagonal and chemical exchange cross-peaks depend on the magnitudes of the longitudinal relaxation rate and the rate constant for the bridge reversal, as well as upon the mixing time chosen in the NOESY experiment. For an equally populated two-site exchange (as here), the integrated volumes of the diagonal and cross peaks may be used to directly calculate the rate constant for the bridge reversal according to eq 1.<sup>11</sup>

$$k = \frac{1}{2\tau_m} \ln \left( \frac{a_d + a_x}{a_d - a_x} \right) \quad (1)$$

In eq 1  $\tau_m$  is the mixing time and  $a_d$  and  $a_x$  are the diagonal and cross-peak volumes in arbitrary units. Equation 1 is valid provided the exchanging nuclei have the same longitudinal relaxation rate, experimentally verified for H<sub>1</sub> and H<sub>10</sub>.

We have obtained 2D exchange spectra at 300, 310, and 320 K and measured the diagonal volume for H<sub>1</sub> as well as the cross-peak volumes connecting H<sub>1</sub> and H<sub>10</sub>. The results are listed in Table 2, along with the calculated rate constant and the activation free energy calculated from the Eyring equation. The reported cross-peak volume is the average of the two measured volumes, found at each temperature to be within a few percent of each other. The activation free energy is seen to be virtually independent of temperature over a 20 K range, indicating a negligible activation entropy associated with the reversal process.

## Discussion

At 300 K, the bridge reversal rate of 0.07 s<sup>-1</sup> corresponds to only four inversions per minute, an exceedingly slow process which is nevertheless detectable by 2D exchange spectroscopy owing to the comparably slow rate of longitudinal relaxation of the exchanging ferrocenyl hydrogens. The barrier is virtually identical with that for the unsubstituted parent compound<sup>3,4</sup> measured by line shape analysis, for which a slightly negative activation entropy of -2.8 eu was reported. Apparently, the *n*-butyl group at the 3-position exerts no significant

(11) Jeener, J.; Meier, B. H.; Bachmann, P.; Ernst, R. R. *J. Chem. Phys.* **1979**, *71*, 4546.

steric or inductive effect on the bridge reversal rate, which is enthalpically driven.

The synthesis of 3-*tert*-butyl-[3]-trithiaferrocenophane has recently been reported,<sup>8</sup> and it too exhibits 14 <sup>1</sup>H ferrocenyl resonances in slow exchange. No kinetic data for the bridge reversal was provided, so the effect on the reversal rate of the bulkier *tert*-butyl substituent at the 3-position is not known. A recent study<sup>12</sup> employing 2D exchange spectroscopy investigated the effect of the metal atom on the reversal rate in unsubstituted [3]-trithiaferrocenophane, with the barrier rising somewhat upon replacement of iron with ruthenium or osmium. This was taken as evidence for a transition-state structure with staggered cyclopentadienyl rings rather than one with eclipsed rings and a planar S<sub>3</sub> bridge. It is perhaps not surprising that the 3-*n*-butyl substituent exerts no significant effect upon the barrier height, as it poses no steric restrictions to the reversal process nor does it interact electronically with the  $\pi$  system of the ferrocene. We are presently investigating the inversion kinetics of the 2-*n*-butyl isomer, for which a substantial steric interaction with the trisulfide bridge is expected.

### Experimental Section

**Synthesis.** The synthesis of 3-*n*-butyl-[3]-trithiaferrocenophane was accomplished as previously described.<sup>13</sup>

**NMR Spectroscopy.** All NMR experiments were carried out on a Bruker DRX-300 NMR spectrometer operating at a <sup>1</sup>H frequency of 300.13 MHz and a temperature of 300 K unless otherwise noted. The system was equipped with a BDTC variable-temperature unit accurate to 0.1 °C, as determined with an ethylene glycol thermometer. 3-*n*-Butyl-[3]-trithia-

ferrocenophane was prepared as a ca. 50 mM solution in toluene-*d*<sub>6</sub>. <sup>13</sup>C spectra employing 1 Hz of line broadening were acquired with a 5 mm broad-band probe. A 5 mm inverse triple-resonance probe was used to acquire <sup>1</sup>H spectra and the HMQC, TOCSY, and NOESY data. One-dimensional <sup>1</sup>H spectra utilized a 5 ppm spectral window, 64k data points, and a 20 s interpulse delay to allow for complete relaxation and were apodized with 0.1 Hz of line broadening. Spectra were base line corrected using Bruker Xwin-nmr 1.2 subroutines prior to integration. The <sup>1</sup>H-detected phase-sensitive <sup>1</sup>H-<sup>13</sup>C chemical shift correlation spectrum was measured at 300 K via the method of Bax and Subramanian<sup>14</sup> using a BIRD pulse sequence<sup>15</sup> to minimize proton magnetization bound to <sup>12</sup>C with an empirically adjusted delay of 900 ms. Spectral windows of 100 and 5 ppm were employed for <sup>13</sup>C and <sup>1</sup>H with a <sup>1</sup>H data block size of 1K, 128 *t*<sub>1</sub> increments, eight scans per increment, and zero-filled to 512 prior to Fourier transformation. Decoupling of <sup>13</sup>C during <sup>1</sup>H acquisition was accomplished with a GARP sequence.<sup>16</sup> The TOCSY experiment was carried out with a spinlock interval of 250 ms, adjusted to account for the small value of *J*<sub>HH</sub> in the ferrocenophane (~2 Hz), and the NOESY experiment employed mixing times of 2.5 s (300 K), 2.0 s (310 K), and 1.5 s (320 K). The relaxation time in the NOESY experiment was set to 15 s to account for the *T*<sub>1</sub> of the ferrocenyl ring protons.

**Acknowledgment** is made to the donors of the Petroleum Research Fund, administered by the American Chemical Society, for the support of this research. Purchase of the NMR spectrometer system was made possible with funds from the National Science Foundation.

OM9710881

(12) Abel, E. W.; Long, N. J.; Orrell, K. G.; Osborne, A. G.; Sik, V. *J. Organomet. Chem.* **1991**, *419*, 375.

(13) Compton, D. L.; Brandt, P. F.; Rauchfuss, T. B.; Rosenbaum, D. F.; Zukoski, C. F. *Chem. Mater.* **1995**, *7*, 2342.

(14) Bax, A.; Subramanian, S. *J. Magn. Reson.* **1986**, *67*, 565.

(15) Garbow, J. R.; Weitekamp, D. P.; Pines, A. *Chem. Phys. Lett.* **1982**, *93*, 504.

(16) Shaka, A. J.; Barker, P. B.; Freeman, R. *J. Magn. Reson.* **1985**, *64*, 547.